Association between retinal and cortical impairments in schizophrenia with visual hallucinations : an electrophysiological study of the visual processing

Irving Remy (irving.remy@outlook.fr)
Institut national de la santé et de la recherche médicale, Unité de recherche INSERM 1114, Université de Strasbourg

Florent Bernardin
Institut national de la santé et de la recherche médicale, Unité de recherche INSERM 1114, Université de Strasbourg

Fabienne Ligier
Centre Universitaire de Psychiatrie de l'Enfant et de l'Adolescent

Julien Krieg
Institut national de la santé et de la recherche médicale, Unité de recherche INSERM 1114, Université de Strasbourg

Louis Maillard
Université de Lorraine, Centre de recherche en automatique de Nancy

Raymund Schwan
Université de Lorraine, IADI, INSERM U1254

Thomas Schwitzer
Université de Lorraine, IADI, INSERM U1254

Vincent Laprévote
Institut national de la santé et de la recherche médicale, Unité de recherche INSERM 1114, Université de Strasbourg

Article

Keywords: Schizophrenia, ERG-EEG, Visual Evoked Potentials, P100, N95, Visual Hallucinations

Posted Date: July 18th, 2022

DOI: https://doi.org/10.21203/rs.3.rs-1593715/v1

Abstract

Electrophysiological deficits in the visual cortical processing are reported in schizophrenia. Specifically, studies support the hypothesis of a magnocellular impairment in the psychiatric illness. However, recent findings reported electrophysiological anomalies as early as retina. Hence, question arises about the link between these retinal and cortical alterations, especially during magnocellular biased conditions among patients with schizophrenia. Their association with visual symptoms such as visual hallucinations was also investigated in this population.

We recorded the P100 amplitude and latency in EEG during the projection of low or high spatial frequency gratings (LSF or HSF ; 0.5 or 15 cycles/degree) presented statically or dynamically (Temporal Frequency TF : 0Hz or 8Hz). We recruited 29 healthy controls (HC, n = 29) and 21 patients with schizophrenia (SZ, n = 21) divided in two subgroups according to the presence or absence of history of visual hallucinations : VH group (n = 9) and auditory hallucinations or no hallucinations group (AHNH group, n = 12). We compared P100 results to former results regarding retinal ganglion cells activity (N95) and visual cognition performances in participants [1]. Data were compared between groups by repeated measures ANCOVA, linear regression analyses and mediation analyses.

First, analysis showed a decreased P100 amplitude and an increased P100 latency in SZ compared to HC ($p < 0.05$). Second, analysis reported main effects of SF and TF without group interaction. More, P100 latency was correlated with the VOSP object score and the N95 latency in SZ group. Third, VH group reported an increased P100 latency compared to HC ($p < 0.05$). P100 latency was also correlated with the VOSP object score and the N95 latency in the VH group. Finally, we found a partial mediation between the P100 latency, N95 latency and VOSP object score in the VH group.

P100 alterations in SZ are consistent with the early visual cortical processing deficit shown in literature. Importantly, these deficits seem to be not related with the magnocellular processing but appears to be associated with previous retinal measurements. Thereby, impairments in N95 and P100 were found only in VH group and were associated with the VOSP object score, thus supporting the role of retina in VH. Studies with coupled ERG-EEG measures are now required to clarify these findings.

1. Introduction

Sensory distortions are an integral part of the complex experience of schizophrenia [2]. Concerning vision, this point has been reported since the first descriptions of Kraepelin and Bleuler [3], and is also commonly described in patients' first-person accounts [4]. Thereby, visual symptoms such as visual hallucinations (VH) are involved in at least 27% of patients [5]. Knowledge of visual function being particularly developed over the last decades, vision sciences reported numerous visual processing anomalies in schizophrenia such as contrast sensitivity [6], visual reading [7], color vision [8], and recognition in objects, images and faces [9–11]. In that sense, electrophysiology, and notably visual evoked potentials (VEP) is a key method to highlight the nature of such visual deficits. Numerous studies reported a decreased P100 amplitude in

schizophrenia at the cortical level [12,13] during various low-level visual tasks such as contour processing [14], fragmented images [15] and simple stimuli perception [16], which also emphasized deficits in the processing of the first visual cortical areas in schizophrenia [17]. More precisely, P100 impairments were found in response to low spatial frequency (LSF) information [18–23] and stimuli biased toward the magnocellular visual system [24,25]. Although such potential magnocellular alteration is well supported in schizophrenia, this theory remains controversial [26], thus challenging the origin of P100 alterations.

Besides, the literature reports both functional and architectural retinal abnormalities in schizophrenia [27,28]. Using flash electroretinography (f-ERG), Balogh et al. [29] reported a decrease in a-wave amplitude in the acute stage of the disease, emphasizing an alteration in the cone response. On a larger sample, Hébert et al. [30] showed a decrease in the amplitude of scotopic b-wave, both photopic a-b-waves, and an increase in the peak time of the b-wave among 105 patients with schizophrenia than 150 controls. Demmin et al. [31] also reported both alterations in the photopic and scotopic conditions with regard to the a-wave as well as the b-wave in these patients. More recently using pattern electroretinography (PERG) [32], our team reported a longer N95 latency in patients with schizophrenia than controls [1]. As the N95 represents almost exclusively the retinal ganglion cell (RGC) activity [33,34] and is considered to be the best marker of these cells [35,36], this result hence provides strong evidence for a delay in the retinal visual transmission caused by RGC dysfunction. This RGC dysfunction was also supported by Moghimi et al. [28] and Demmin et al. [37] by using the photonegative response (PhNR) in f-ERG. Finally, Samani et al. 2018 [27] found a decrease in the retinal contrast sensitivity regarding to LSF, correlated with thinning of the parafoveal and temporal RGC complex in schizophrenia. Since RGC are divided into M and P cells at the retinal level [38], authors hypothesized that these alterations may signify a disease-related loss of magnocellular ganglion cells which could recall the magnocellular alteration at the cortical level. In sum, these results highlight abnormalities in retinal synaptic transmission, affecting both photoreceptors as well as RGC functions. As RGC constitutes the first link with the input of subsequent brain regions such as the primary visual cortex (PVC) [38–40], and since retinal and cerebral neurons share similar anatomical and functional properties [41], impaired retinal functions may affect signaling at the subcortical and cortical levels [42].

Indeed, it is important to note that retinal abnormalities could affect the visual cortical processing in ophthalmic diseases [43] and neurodegenerative disorders [44,45]. For instance, using pattern VEP and PERG, Krasodomska et al. 2010 [46] reported an increased P50 latency, a decrease in N95 and P50 amplitudes, and an increased P100 latency in 30 patients with early stage of Alzheimer disease. Similarly, Heravian et al. 2011 [47] found reductions in the P50 and P100 amplitudes and an increased P100 latency in patients with anisometropic amblyopia. More recently, El-Shazly et al. [48] reported an increased N95 latency, a decrease in N95 amplitude, a prolonged P100 latency and a decreased P100 amplitude in patients with migraine during aura. Such results emphasized that retinal abnormalities may have consequences on the visual cortical processing and especially the P100 wave. With that in mind, our group explored in a past study the retinal function in patients with schizophrenia with and without history of VH [1] and found that

the N95 would be associated to VH and high-level visual cognition [49]. In such a way, the question arises to elucidate the relationship between retinal dysfunctions and the subsequent visual processing in schizophrenia and notably in patients with a history of VH. First, exploring P100 activities in these patients compared with healthy controls could be a way to find the deficit in the early visual cortical processing mentioned in literature. Second, the use of a method such as VEP in EEG remains yet to explore in these populations. Finally, this could be the opportunity to increase our understanding about the effect of VH at the cortical level and to determine if there is a possible link between retinal and cortical abnormalities as well as high-level visual cognition.

On this purpose, the primary goal of this study was to explore the visual cortical processing among patients with schizophrenia compared to healthy controls. We used P100 activities in EEG such as amplitude and latency in response to spatial frequency gratings stimuli to bias either the magnocellular or parvocellular visual activity [50,51]. Based on previous literature, we hypothesized P100 alterations specifically on magnocellular biased stimuli. We also considered a potential link between previous PERG results [1] and EEG measurements in the schizophrenia group. A secondary aim was to explore the link between cortical and retinal electrophysiological abnormalities as well as visual symptoms such as VH in patients with and without a history of VH. We hypothesized P100 alterations in patients with a history of VH and a complex interaction between previous PERG measurements [1], EEG measurements and visual hallucinations in this group.

2. Material And Methods

2.1. Clinical assessments and participants ethics statement

This study is a part of the CAUSAMAP project (Cannabis USe And MAgnocellular Processing) which aims at studying the neurotoxic effect of cannabis on human vision. We initially planned to recruit 30 patients with schizophrenia and 30 age-/sex- matched healthy controls. However, not all EEG plots were usable due to missing EEG data or too much artifact recording. So, final recruitment consisted in 21 patients with schizophrenia (n = 21, mean $_{age}$= 29yo, standard deviation (SD = 8.15 years) and 29 healthy controls (n = 29, mean $_{age}$= 25.89yo, SD = 5.49 years). All participants were between 19 and 46 years old. They provided a detailed psychoactive drug and their medical history. They had a normal fundoscopic examination and a normal or corrected-to normal visual acuity verified by the Monoyer chart. All participants had a general psychiatric assessment using the MINI 5.0 [52]. Alcohol or cannabis disorder were not an exclusion criterion to facilitate recruitment. Patients with an Alcohol Use Disorders Identification Test (AUDIT) and Cannabis Abuse Screening Test (CAST) indicating alcohol or cannabis dependence were excluded.

Patients with schizophrenia fulfilled the DSM IV-TR Axis I Disorders criteria for schizophrenia. Current (past month) and lifetime visual and auditory hallucinations were assessed using the Psycho-Sensory hAllucination Scale (PSAS). The PSAS provides an index of the gravity of the hallucinations and

represents the sum of scores for the clinical characteristics of hallucinations such as frequency, duration, negative aspects, conviction, impact, control and sound intensity (for auditory hallucinations) [53]. Patients were therefore divided into two subgroups according to the absence or presence of a history of visual hallucinations measured with the PSAS. Therefore, 9 patients had an history of VH (VH group : n = 9, mean $_{age}$= 30.11yo, SD = 9.47 years) and 12 patients had an history of auditory hallucinations or no hallucinations (AHNH group : n = 12, mean $_{age}$= 28.17yo, SD = 7.33 years). There were clinically stable on antipsychotic medication and had no history of neurologic disease. They presented a negative urine toxicology test for illicit drug or opiate substitution treatment use. Healthy controls had no actual or past psychiatric disorder, no family or personal history of schizophrenia or bipolar disorder, no history of neurological disease, no alcohol or THC dependance, no trouble meeting the DSM IV (Diagnostic and Statistical Manual of Mental Disorders IV) and no history of ophthalmic disease or visual symptoms.

Participants received €100 in vouchers (about US$110). They signed informed consent detailing all aspects of research in compliance with the Helsinki declaration [54]. All experiments were performed in accordance with the ethics committee of Nancy Regional University Hospital Center (2013-A00097-38 CPP 13.02.02). The study was first registered on August 12, 2016 and is available on clinicaltrials.gov (ID NCT02864680).

2.2. Neuropsychological assessment

This method description was previously made by our team in Bernardin et al. 2019 [49]. Thus, a French version of the following neuropsychological tests were administered to evaluate specific cognitive field of the participants : National Adult Reading Test [55]; the California Verbal Learning Test [56]; the verbal fluency test [57]; working memory, Go/No-go and divided attention subtests of the Test of Attentional Performance [58]; coding subtest of the Wechsler Adult Intelligence Scale [59] and the VOSP battery [60]. The VOSP battery has two indices : the VOSP-Object index, which groups subtests that evaluate shape and object recognition, and the VOSP-Space index, which groups subtests that evaluate spatial relationships of both 2D and 3D objects.

2.3. Experimental procedure, recording and EEG data processing

This method description was previously realized by our team in Remy et al. 2021 [61]. Stimuli were generated using the VSG system (Cambridge Research System). They consisted in black and white sinusoidal vertical Gabor gratings presented at a size of 6 degrees of visual angle [51]. We choose LSF and High Spatial Frequency (HSF) gratings (0.5 and 15 cycles per degree respectively) in order to preferentially stimulate magnocellular and parvocellular pathway [62,63]. The gratings had a light/dark contrast of 80% and were presented against an isoluminant grey field. Both types of gratings were presented at two different temporal frequency (TF) conditions. In dynamic condition (which preferentially stimulates the magnocellular pathway activity [64]), black and white stripes alternated at a frequency of 8Hz. In static condition, the stripes did not alternate (0Hz). 20% of the stimuli were control stimuli at a

contrast of 0% and were invisible. Five stimuli were used : LSF-static, LSF- dynamic, HSF-static, HSF-dynamic and control stimuli.

Figure 1 shows experimental procedure with both stimuli in LSF and HSF. A total of 300 stimuli were projected onto a CRT screen with a sampling rate of 120Hz, in an electrically shielded room with no surrounding light. The participants sat on a chair at a distance of 57 cm. During each trial, a central fixation cross was displayed during 500ms to 800ms and allowed participants to maintain their attention in the central zone of the screen. A randomized grating presentation was then centrally presented for 500ms. During the following blank screen lasting 1500ms, participants had to indicate via a response button if they had seen a grating. This task aimed to maintain the attention of the participants on the stimuli. Each trial was separated by a supplementary blank of 1500ms. The entire procedure consisted of 300 trials in total with 60 trials per stimulus condition and was divided into 2 blocks of 150 trials.

[Insert Fig. 1 here]

EEG recording was performed by Ag/AgCl electrodes using a 64-electrode Micromed® headset (10–10 system, QuickCap ; Compumedics Neuroscan®) referenced to both ear lobes. The signal was recorded at a sampling rate of 512 Hz (SD64 Headbox, Micromed®, Italy) with a bandwidth from 0.15Hz to 200Hz. Electrode impedances were kept below 10 kΩ. Vertical and horizontal ocular electrodes were used for eye-artifact rejection. Each epoch was created with 1000ms pre-stimulus and lasted for 1000ms post-stimulus for each modality of spatial frequency (SF) relative to the stimulus onset. The data acquired were processed with Brain Vision Analyzer 2.0® software (Brain Products GmbH, Munich, Germany). The raw EEG signal was bandpass-filtered (0.5Hz-40Hz). Artifact rejection for noise, eyes blinking, muscular activity and non-biological component was performed using independent component analysis (ICA)[65]. A manual artifact rejection was based on visual inspection to exclude the last remaining artifacts. Data collection focused on 3 pairs of interest electrodes in the left (O_1, PO_3, PO_7) and the right hemisphere (O_2, PO_4, PO_8). A grand average on all conditions determined the global aspect of P100 amplitude peak. A root mean square (RMS) value calculation determined a temporal window for the extraction of the P100 component amplitude. Consequently, the P100 peak was extracted with a 28ms interval around the maximum peak. P100 latency was extracted based on its mean appearance on the grand average. Therefore, P100 latency was determined at 116ms for patients with schizophrenia and 113ms for healthy controls.

2.4. Experimental procedure, recording and ERG data processing

Detailed information about the stimulation and recording processes are described in Schwitzer et al. [66]. Briefly, we used the MonPackOne system (Metrovision) for stimulations, recording and analysis. The exploration of RGC functions was performed using reversal checkerboards stimuli according to ISCEV standards [36]. PERG markers were the N95 and P50 waves.

2.5. Statistical analysis

This paragraph was previously described by our team in Remy et al. 2021 [61]. Data were analyzed using STATISTICA software (version 10.0) and R (version 4.0.5.). Both descriptive and comparative analyses were conducted according to the nature and the distribution of the variables (normality assessed by Shapiro-Wilk test). Qualitative variables are described with frequencies and percentages ; quantitative variables were reported with the mean and standard deviation (SD). Since sociodemographic and clinical characteristics followed a normal distribution given the non-significant Shapiro-Wilk test, the differences between groups were analyzed using an independent sample t-test. Given behavioral and EEG data followed a normal distribution, indicated by a non-significant Shapiro-Wilk test, and did not differ in variances following a non-significant Levene test, we used parametric tests. Behavioral data consisted of 2*2 factors ANOVA (TF [Dynamic/Static] x SF [LSF/HSF]). P100 amplitude and latency were analyzed using 2*3*2*2 factors ANOVA (Hemisphere [left/right] x Electrodes [$O_{1/2}$, $PO_{3/4}$, $PO_{7/8}$] x TF [dynamic/static] x SF [LSF/HSF]). Pearson R- tests assessed correlations between experimental variables. More information for PERG statistical analysis was given in Bernardin et al. 2019 (1). A mediation analysis using structural equation model [67] was made between PERG measurements, EEG measurements and the VOSP index score. For all tests, the significance was $\alpha = 0.05$.

3. Results

3.1. Comparison between patients with schizophrenia (SZ) and healthy controls (HC)

3.1.1. Population characteristics

Sociodemographic and clinical characteristics of the participants are summarized in Table 1. Among the 21 patients with schizophrenia, 2 were cannabis users and 12 were alcohol users without dependance.

[Insert Table 1 *here]*

3.1.2. Behavioural data

SZ and HC displayed respectively a mean reaction time of 595.15ms (SD = 46.60ms) and 393.01ms (SD = 14.87ms). ANOVA analysis showed a significant main group effect ($F(1,47) = 22.98$; $p < 0.01$) indicating a higher mean reaction time in SZ patients compared to HC regardless the type of stimuli.

3.1.3. EEG results

P100 amplitude

The mean P100 amplitude in SZ and HC was respectively 2.25µV (SD = 0.52µV) and 3.42µV (SD = 0.62µV). ANOVA showed a main group effect ($F(1,48) = 7.88$; $p < 0.01$) indicating a lower P100 amplitude in SZ compared to HC (Fig. 2).

[Insert Fig. 2 here]

A main SF effect (F(1,48) = 51.34 ; $p < 0.001$) highlighted a larger P100 amplitude for LSF gratings (mean = 3.80µV ; SD = 1.94µV) compared to HSF gratings (mean = 1.89µV ; SD = 1.49µV). The interaction SF*Group was not significant (F(1,48) = 0.04 ; $p = 0.85$). Analysis indicated a main TF effect (F(1,48) = 8.79 ; $p < 0.01$) explained by a greater P100 amplitude for Dynamic condition (mean = 3.02µV ; SD = 1.51µV) compared to Static condition (mean = 2.67µV ; SD = 1.49µV). The TF*Group interaction was not significant (F(1,48) = 1.17 ; $p = 0.29$). No main effect was found elsewhere.

P100 latency

The mean P100 latency in SZ and HC was respectively 117.04ms (SD = 2.65ms) and 112.46ms (SD = 2.31ms). ANOVA showed main group effect (F(1,48) = 6.45; $p < 0.05$) indicating an increase in P100 latency in SZ than HC (Fig. 3).

[Insert Fig. 3 here]

Analysis exhibited a main SF effect (F(1,48) = 17.89 ; $p < 0.001$) explained by a shorter P100 latency for LSF gratings (mean = 112.72ms ; SD = 7.04ms) than HSF gratings (mean = 116.72ms ; SD = 6.85ms). The SF*Group interaction was not significant (F(1,48) = 0.34 ; $p = 0.56$). No main effect was found elsewhere.

P100 correlation analysis

In the SZ group, the P100 latency was negatively correlated with the VOSP-Object score (n = 21 ; r=-0.52 ; $p < 0.05$). Thus, the higher the P100 latency in SZ, the lower the VOSP object score. No correlations in either the SZ or HC group were found between P100 amplitude or latency on the one hand (n = 50 ; r=-0.01; $p = 0.92$) and between P100 amplitude or latency and CAST score, AUDIT score or number of joints per week on the other hand ($p > 0.05$).

3.1.4. PERG results

PERG results were described previously in Bernardin et al 2019 [1] and are in the supplementary material. The main result was a significant effect of group for N95 latency (F(1,54) = 18.0 ; $p < 0.001$) indicating an increase in N95 latency in SZ (mean = 95.7ms ; SD = 7.5ms) than HC (mean = 88.4ms ; SD = 5.4ms).

3.1.5. Association between EEG results and previous PERG results

We found a positive correlation between the N95 latency and the P100 latency in the SZ group (n = 21 ; r = 0.85 ; $p < 0.05$). Thus, the higher the N95 latency, the higher the P100 latency in the SZ group. No other significant correlations were found elsewhere ($p > 0.05$).

3.2 Comparisons between patients with schizophrenia and VH (VH), patients with schizophrenia and auditory

hallucinations or no hallucinations (AHNH) and healthy controls (HC).

3.2.1. Population characteristics

Sociodemographic and clinical characteristics of the participants are summarized in Table 2.

[Insert Table 2 *here]*

3.2.2. Behavioural data

HC, VH and AHNH group displayed respectively a mean reaction time of 389.11ms (SD = 22.08ms), 549.66ms (SD = 43.86ms) and 632.45ms (SD = 75.92ms). ANOVA analysis evidenced a significant main group effect ($F(2,46) = 12.42$; $p < 0.01$) indicating a higher mean reaction time in VH ($F(1,36) = 17.86$; $p < 0.01$) and AHNH group ($F(1,38) = 21.15$; $p < 0.01$) compared to HC regardless the type of stimuli.

3.2.3. EEG results

P100 amplitude

The mean P100 amplitude in HC, VH group and AHNH group and was respectively 3.42µV (SD = 0.30µV), 2.84µV (SD = 0.41µV) and 1.84µV (SD = 0.22µV). ANOVA showed a group factor effect ($F(2,47) = 5.28$; $p < 0.01$). Analysis indicated a decrease in P100 amplitude in the AHNH group compared to both VH group ($p < 0.05$) and HC ($p < 0.01$)(Fig. 4).

[Insert Fig. 4 here]

A main SF effect ($F(1,47) = 41.74$; $p < 0.001$) indicated that P100 amplitude was greater in the LSF gratings (mean = 3.67µV ; SD = 2.14µV) than HSF gratings (mean = 1.73µV ; SD = 1.63µV). The SF*Group interaction was not significant ($F(2,47) = 0.05$; $p = 0.95$). Analysis indicated a main TF effect ($F(1,47) = 5.04$; $p < 0.05$) explained by a greater P100 amplitude for Dynamic condition (mean = 2.85µV ; SD = 1.64µV) than Static condition (mean = 2.55µV ; SD = 1.65µV). The TF*Group interaction was not significant ($F(2,47) = 0.75$; $p = 0.48$).

P100 latency

The mean P100 latency in HC, VH and AHNH group was respectively 112.46ms (SD = 0.98ms) ; 117.41ms (SD = 2.11ms) and 116.63ms (SD = 2.01ms). ANOVA showed a group factor effect ($F(2,47) = 3.20$; $p < 0.05$). Interestingly, analysis indicated an increase in P100 latency in VH compared to HC ($F(1,36) = 4.74$; $p < 0.05$) but not on other comparisons ($p > 0.05$) (Fig. 5).

[Insert Fig. 5 here]

A main SF effect (F(1,47) = 16.29 ; $p < 0.001$) showed a shorter P100 latency for LSF gratings (mean = 113.45ms ; SD = 7.9ms) than HSF gratings (mean = 117.55ms ; 7.51ms). The SF*Group interaction was not significant (F(2,47) = 2.45 ; $p = 0.10$).

P100 correlations in SZ subgroups

The P100 latency was negatively correlated with the VOSP object score (n = 9 ; r=-0.63 ; $p < 0.01$) in the VH group, but not in the AHNH group (n = 12, r=-0.46 ; $p = 0.14$). Thus, the lower the VOSP object score, the higher the P100 latency in the VH group. No correlations in either the AHNH, VH or HC group were found between P100 amplitudes or latency on the one hand and between P100 amplitudes or latency and CAST score, AUDIT score or number of joints per week on the other hand ($p > 0.05$).

3.2.4. PERG results

PERG results were described previously in Bernardin et al 2019 [1] and are in the supplementary material. One of the main results concerned a significant effect of group for N95 latency (F(2,54) = 10.5, $p < 0.0001$) where post-hoc Tukey test revealed a strong trend towards an increased N95 latency in the VH group compared to HC ($p \sim 0.06$).

3.2.5. Association between EEG results and previous PERG results

Pearson's analysis showed a positive correlation between the mean N95 latency and the mean P100 latency in VH only (n = 9; r = 0.71 ; $p < 0.05$). Thus, the higher the N95 latency, the higher the P100 latency in the VH group. No other significant correlations were found elsewhere between the N95 or P50 and the P100 ($p > 0.05$).

3.3. Mediation analysis between EEG results and previous PERG results [1]

The primary visual cortex (PVC) extends to pre-striated areas such as the ventral visual pathway, which could be reflected by the VOSP object score [68]. So, we made further regression analysis integrating the N95 latency, the P100 latency and the VOSP object score to investigate the potential link between retinal abnormalities, cortical abnormalities, and high-level visual cognition.

A first linear regression equation showed a significant relationship between the N95 latency and the VOSP object score in the VH group (n = 9, F(1,7) = 18; r=-0.31 ; $p < 0.01$). A second linear regression showed a significant association between [1] [N95 latency - P100 latency](n = 9 ; r = 0.77; $p < 0.05$) and [2] [P100 latency - VOSP object score](n = 9, r=-0.14 ; $p < 0.05$).

Given the continuity of visual pathways, the P100 latency could therefore be considered as a mediator for the N95 latency onto the VOSP score in patients with VH. According to this model, we found with a partial mediation analysis a significant standardized estimate of the causal paths for the direct effect [N95

latency- VOSP object score] when including the mediator [P100 latency] in the equation (n = 9 ; r=-0.26 ; *p* < 0.01). The summary of the paths with coefficients which presented this mediation model is presented in Fig. 6.

[Insert Fig. 6 here]

We found no significant differences for linear regression performed on the SZ group or in the other groups (AHNH or HC group) (p > 0.05).

4. Discussion

This study aimed to explore the visual cortical processing among patients with schizophrenia compared to healthy controls and to explore its link with previous retinal electrophysiological processing and visual cognition such as visual hallucinations. First, we found a decreased P100 amplitude and an increased P100 latency in SZ compared to HC. Importantly, these results were independent of either SF or TF nature of the stimuli. In the SZ group, P100 latency was correlated with the VOSP object score and previous retina results such as N95 latency [1]. Third, P100 amplitude was decreased in AHNH compared to both VH and HC and P100 latency was increased in VH compared to HC. In the VH group, P100 latency was correlated with the VOSP object score and previous retina results such as the N95 latency [1]. Finally, a mediation analysis reported both causal and temporal relations between retinal and cortical measures as well as visual cognitive abnormalities in VH group, shown by a longer N95 latency, a longer P100 latency and weaker performances in the VOSP object score.

Our primary goal was to explore the visual cortical processing among patients with schizophrenia compared to healthy controls. Thereby, we found P100 alterations in the SZ group, which are consistent with the most studies which refers to impairments in the very first step of the early visual cortical processing and notably the primary visual cortex [69,70]. Analysis also mentioned a higher P100 amplitude and shorter P100 latency for LSF stimuli and dynamic condition [19,21–23], consistent with the magnocellular sensitivity to LSF information and movements [64]. Despite, our analysis failed to find any SF*Group interaction or TF*Group interaction. Such results hence undermine this potential magnocellular alteration in schizophrenia although well described in the literature. For instance, Butler et al. [22] reported a P100 reduction in response to magnocellular biased stimuli with gratings very similar to those in this present study. Nevertheless, and compared to our study, their patients were older (35.9 ± 2.2 years vs. 29 ± 8.15 years in our study), with a duration of illness twice as long (16.7 ± 1.8 years vs. 94.67 ± 93.21 months in our study) and chlorpromazine equivalent rates nearly three times higher (1365.4 ± 157.7 mg/day vs. 544.55 ± 241.29 mg/day in our study). In this regard, literature mentions that visual abnormalities in schizophrenia may be more pronounced with age, duration, stage, and severity of the illness (Joseph 2013). Similarly, the use of antipsychotic medications may impair visual performance, including contrast perception, to a greater extent than without the use of antipsychotic medication [8,71]. In sum, several factors could have an influence on this potential magnocellular alteration listed in schizophrenia, which would be less visible here in our patients.

If our results are not conditioned by the use of visual stimuli preferentially oriented towards the magnocellular or parvocellular system, it is important to consider the interaction between retinal and cortical processing. In our paradigm, we found a positive correlation between the N95 latency at the retinal level and the P100 latency at the cortical level in the SZ group. Hence, one hypothesis would be that P100 cortical alterations rather reflect retinal dysfunctions than thalamic magnocellular dysfunctions. This hypothesis also fits with previous studies which have shown that retinal anomalies can have repercussions at the cortical level in ophthalmic and neurological disorders such as anisometropic amblyopia [47], Alzheimer disease [46] and migraine [48], as evidenced by multiple deficiencies on electrophysiological measurements of N95, P50 and P100 waves.

This study also aimed to determine the links between electrophysiological visual abnormalities, both at retinal and cortical level, and the presence or absence of visual symptoms such as VH in schizophrenia. Although electrophysiological abnormalities appear to be present in all subgroups, both at the retinal and cortical level and either in the VH or the AHNH group, the delay at the cortical level appears to follow the delay at the retina level in the VH group, as reflected by a greater N95 latency and a greater P100 latency. Moreover, the P100 delay in the VH group was associated with lower VOSP object-score which is also consistent with our recent retina results mentioning that greater N95 latency was associated with weaker performances at the VOSP score predicted the risk of having VH [49]. In patients with VH, there would therefore be a potential association between the retinal abnormalities, the visual cortical abnormalities and processing in high-level visual cognition such as VH. On this purpose, our mediation analysis performed in the VH group also emphasize cognitive models of VH that hypothesized the role of impaired retinal input as a risk factor for developing VH [72]. For instance, the Activation Input Modulation model proposed by Diederich, Goetz and Stebbins in 2005 [73] hypothesizes that the retina may cause a dysregulation of the input dimension leading to release of internally generated visual images causing VH in Parkinson's disease [74]. This may be consistent with our findings and previous studies linking retinal dysfunction, cerebral dysfunction, and visual symptoms [49,75] and also be applicable here in the VH group for schizophrenia. In sum, one hypothesis could be that patients with VH would be potentially more sensitive to changes in the retinal processing, which impact therefore the visual cortical measures in EEG and the visual clinical performances. However, no existing model are perfectly tailored for VH in schizophrenia as they aim to explain VH in neurological disorders [72] and further research are required to clarify the role of the early visual processing in VH.

The main strength of our study is that our findings are the first to raise potential arguments for a relation between retinal and visual cortical abnormalities in psychosis. More, such results concerning the symptomatology of VH coupled with high-level visual cognition has never been reported. First, this possible link would suggest that retinal anomalies could potentially have repercussions on the visual cortical processing in patients with schizophrenia and VH. This is especially important since our regression analyses integrated the VOSP object score, which assesses perceptual processes independent of potential disease-related cognitive and motor impairments [76,77]. Moreover, electrophysiology provides good objectivity, reliability, and reproducibility in the results, especially during measurements involving

low-level visual stimuli that are poorly sensitive to attentional factors. As VH are associated with a severe psychopathology, a low prognosis [78–80] and a high risk of mortality [81], electrophysiology could be used to study patients in clinic for better therapeutic management.

Our study has also certain limitations. First, our sample sizes were small and additional studies are needed to validate these results on a larger scale. Second, the AHNH group included patients with a history of auditory hallucinations or patients with no history of hallucinations at all. Thus, interpretation of the results on this group was very difficult and further studies are needed among patients with AH only. Third, although there were no differences between groups in terms of clinical characteristics, substance use must be considered. Indeed, Schwitzer et al. [82] found an increase in N95 latency among regular cannabis users. At the cortical level, we recently found a P100 impairment in regular cannabis users in response to the same stimuli to those described in this study [61]. Similarly, smoking nicotine would affect the P100 latency in studies using visual modality tasks [83] and alcohol could also have effects by causing a P100 latency delay, even in healthy subjects [84]. Nevertheless, we did not find any correlations between cannabis or cigarettes, or number of alcohol glasses consumed daily and the P100 results. Moreover, only two patients were cannabis users, and they were not alcohol dependent. Additional studies in patients with schizophrenia without substance use are now necessary. Fourth, although we had the same patients as in our previous retina study [1], stimulations were different for both electrophysiological methods and measures were decoupled. As the stimuli used tested low-level visual processing for both techniques, we assume to compare the retinal and brain measures. However, simultaneous ERG-EEG recordings are now necessary to confirm these results.

5. Conclusion

Understanding the electrophysiological mechanisms underlying visual deficits in psychiatric disorders constitute a scientific challenge since last decades. Our results indicated low-level visual alterations in patients with schizophrenia, consistent with the deficit in the early visual cortical processing in the literature. However, these alterations are apparently not specific to visual stimuli strongly biased towards the magnocellular system, a hypothesis that is very much supported in the psychiatric illness. In fact, these cortical abnormalities seem to be more related to retinal electrophysiological abnormalities as well as to clinical visual performance. Such outcomes also reinforce the role of the retina and visual hallucinations in psychosis and state the first correlates that cortical anomalies could potentially be caused by retinal anomalies in schizophrenia. Further studies with simultaneous and comparable electrophysiological methods are now necessary to confirm the relation between both visual stages. Their particular interest in the psychiatric field could undoubtedly improve the prevention and early detection of psychosis in the clinic.

Declarations

ACKNOWLEDGEMENTS

We thank all members of the CAUSAMAP study group : Éliane Albuisson, Centre Hospitalier Régional Universitaire Nancy; Karine Angioi-Duprez, Service d'ophtalmologie, Centre Hospitalier Régional Universitaire Nancy; Marc Borie, Centre Hospitalier Régional Universitaire Nancy; Stéphanie Caharel, PhD, INTERPSY, Université Lorraine; Paolo Di Patrizio, MD, PhD, Université Lorraine; Anne Giersch, Institut National de la Santé et de la Recherche Médicale U1114, Fédération de Médecine Translationnelle de Strasbourg, Département de Psychiatrie, Centre Hospitalier Régional Universitaire de Strasbourg; Philip Gorwood, MD, PhD, Centre de Psychiatrie et Neurosciences; Coline Jeantet, INTERPSY, Université Lorraine; Julien Krieg, Institut National de la Santé et de la Recherche Médicale U1114, Strasbourg; Laurence Lalanne, Institut National de la Santé et de la Recherche Médicale U1114, Fédération de Médecine Translationnelle de Strasbourg, Département de Psychiatrie, Centre Hospitalier Régional Universitaire de Strasbourg; Joëlle Lighezzolo-Alnot, PhD, INTERPSY, Université Lorraine; Valérie Louis Dorr, MD, PhD, Centre de Recherche en Automatique de Nancy, Centre national de la recherche scientifique, Unité mixte de recherche 7039; Louis Maillard, MD, PhD, Centre de Recherche en Automatique de Nancy, Centre national de la recherche scientifique, Unité mixte de recherche 7039, and Nicolas Ramoz, MD, PhD, Centre de Psychiatrie et Neurosciences, Paris.

CONFLICT OF INTEREST

The authors have no conflict of interest to disclose, either on competing financial or non-financial interests in relation to the work described.

ROLE OF THE FUNDING SOURCE

This study was supported by grant ANR-12-SAMA-0016-01 from the French National Research Agency and by the French Mission Interministérielle contre les Drogues et les Conduites Addictives. The funding sources have no role in the design and conduct of the study; collection, management, analysis, and interpretation of the data; preparation, review, or approval of the manuscript; and decision to submit the manuscript for publication.

References

1. Bernardin, F. *et al.* Retinal ganglion cells dysfunctions in schizophrenia patients with or without visual hallucinations. Schizophr. Res. S0920996419302701 (2019) doi:10.1016/j.schres.2019.07.007.
2. Javitt, D. C. & Freedman, R. Sensory processing dysfunction in the personal experience and neuronal machinery of schizophrenia. Am. J. Psychiatry **172**, 17–31 (2015).
3. Javitt, D. C. When doors of perception close: bottom-up models of disrupted cognition in schizophrenia. Annu. Rev. Clin. Psychol. **5**, 249–275 (2009).
4. Chapman, J. Schizophrenia from the inside. Ment. Health Lond. **25**, 6–8 (1966).
5. Waters, F. *et al.* Visual hallucinations in the psychosis spectrum and comparative information from neurodegenerative disorders and eye disease. Schizophr. Bull. **40 Suppl 4**, S233-245 (2014).

6. Kéri, S., Antal, A., Szekeres, G., Benedek, G. & Janka, Z. Spatiotemporal visual processing in schizophrenia. J. Neuropsychiatry Clin. Neurosci. **14**, 190–196 (2002).
7. Revheim, N. *et al.* Reading impairment and visual processing deficits in schizophrenia. Schizophr. Res. **87**, 238–245 (2006).
8. Fernandes, T. M. P. *et al.* Color vision impairments in schizophrenia and the role of antipsychotic medication type. Schizophr. Res. **204**, 162–170 (2019).
9. Schneider, F. *et al.* Impairment in the specificity of emotion processing in schizophrenia. Am. J. Psychiatry **163**, 442–447 (2006).
10. Klosterkötter, J., Schultze-Lutter, F. & Ruhrmann, S. Kraepelin and psychotic prodromal conditions. Eur. Arch. Psychiatry Clin. Neurosci. **258 Suppl 2**, 74–84 (2008).
11. Oker, A. *et al.* Schizophrenia patients are impaired in recognition task but more for intentionality than physical causality. Conscious. Cogn. **67**, 98–107 (2019).
12. Foxe, J. J., Doniger, G. M. & Javitt, D. C. Early visual processing deficits in schizophrenia: impaired P1 generation revealed by high-density electrical mapping. Neuroreport **12**, 3815–3820 (2001).
13. Butler, P. D. *et al.* Dysfunction of Early-Stage Visual Processing in Schizophrenia. Am J Psychiatry 8 (2001).
14. Foxe, J. J., Murray, M. M. & Javitt, D. C. Filling-in in schizophrenia: a high-density electrical mapping and source-analysis investigation of illusory contour processing. Cereb. Cortex N. Y. N 1991 **15**, 1914–1927 (2005).
15. Doniger, G. M., Foxe, J. J., Murray, M. M., Higgins, B. A. & Javitt, D. C. Impaired visual object recognition and dorsal/ventral stream interaction in schizophrenia. Arch. Gen. Psychiatry **59**, 1011–1020 (2002).
16. Yeap, S. *et al.* Early visual sensory deficits as endophenotypes for schizophrenia: high-density electrical mapping in clinically unaffected first-degree relatives. Arch. Gen. Psychiatry **63**, 1180–1188 (2006).
17. Butler, P. D. & Javitt, D. C. Early-stage visual processing deficits in schizophrenia. Curr. Opin. Psychiatry **18**, 151–157 (2005).
18. Kim, D., Zemon, V., Saperstein, A., Butler, P. D. & Javitt, D. C. Dysfunction of early-stage visual processing in schizophrenia: harmonic analysis. Schizophr. Res. **76**, 55–65 (2005).
19. Obayashi, C. *et al.* Decreased spatial frequency sensitivities for processing faces in male patients with chronic schizophrenia. Clin. Neurophysiol. **120**, 1525–1533 (2009).
20. Kim, D.-W., Shim, M., Song, M. J., Im, C.-H. & Lee, S.-H. Early visual processing deficits in patients with schizophrenia during spatial frequency-dependent facial affect processing. Schizophr. Res. **161**, 314–321 (2015).
21. Lee, J. S., Park, G., Song, M. J., Choi, K.-H. & Lee, S.-H. Early visual processing for low spatial frequency fearful face is correlated with cortical volume in patients with schizophrenia. Neuropsychiatr. Dis. Treat. **12**, 1–14 (2016).

22. Butler, P. D. *et al.* Subcortical visual dysfunction in schizophrenia drives secondary cortical impairments. Brain **130**, 417–430 (2007).
23. Martínez, A. *et al.* Consequences of magnocellular dysfunction on processing attended information in schizophrenia. Cereb. Cortex N. Y. N 1991 **22**, 1282–1293 (2012).
24. Schechter, I. *et al.* Impairments in generation of early-stage transient visual evoked potentials to magno- and parvocellular-selective stimuli in schizophrenia. Clin. Neurophysiol. Off. J. Int. Fed. Clin. Neurophysiol. **116**, 2204–2215 (2005).
25. Knebel, J.-F., Javitt, D. C. & Murray, M. M. Impaired early visual response modulations to spatial information in chronic schizophrenia. Psychiatry Res. **193**, 168–176 (2011).
26. Skottun, B. C. & Skoyles, J. R. Contrast sensitivity and magnocellular functioning in schizophrenia. Vision Res. **47**, 2923–2933 (2007).
27. Samani, N. N. *et al.* Retinal Layer Abnormalities as Biomarkers of Schizophrenia. Schizophr. Bull. **44**, 876–885 (2018).
28. Moghimi, P. *et al.* Electoretinographic evidence of retinal ganglion cell-dependent function in schizophrenia. Schizophr. Res. **219**, 34–46 (2020).
29. Balogh, Z., Benedek, G. & Kéri, S. Retinal dysfunctions in schizophrenia. Prog. Neuropsychopharmacol. Biol. Psychiatry **32**, 297–300 (2008).
30. Hébert, M. *et al.* Light evoked potentials measured by electroretinogram may tap into the neurodevelopmental roots of schizophrenia. Schizophr. Res. **162**, 294–295 (2015).
31. Demmin, D. L., Davis, Q., Roché, M. & Silverstein, S. M. Electroretinographic anomalies in schizophrenia. J. Abnorm. Psychol. **127**, 417–428 (2018).
32. McCulloch, D. L. *et al.* ISCEV Standard for full-field clinical electroretinography (2015 update). Doc. Ophthalmol. **130**, 1–12 (2015).
33. Froehlich, J. & Kaufman, D. I. The pattern electroretinogram: N95 amplitudes in normal subjects and optic neuritis patients. Electroencephalogr. Clin. Neurophysiol. **88**, 83–91 (1993).
34. Hull, B. M. & Thompson, D. A. A review of the clinical applications of the pattern electroretinogram. Ophthalmic Physiol. Opt. J. Br. Coll. Ophthalmic Opt. Optom. **9**, 143–152 (1989).
35. Holder, G. E. *et al.* International Federation of Clinical Neurophysiology: recommendations for visual system testing. Clin. Neurophysiol. Off. J. Int. Fed. Clin. Neurophysiol. **121**, 1393–1409 (2010).
36. Bach, M. *et al.* ISCEV standard for clinical pattern electroretinography (PERG): 2012 update. Doc. Ophthalmol. **126**, 1–7 (2013).
37. Demmin, D. L., Netser, R., Roché, M. W., Thompson, J. L. & Silverstein, S. M. People with current major depression resemble healthy controls on flash Electroretinogram indices associated with impairment in people with stabilized schizophrenia. Schizophr. Res. **219**, 69–76 (2020).
38. Webvision: *The Organization of the Retina and Visual System*. (University of Utah Health Sciences Center, 1995).

39. Holder, G. E. Pattern electroretinography (PERG) and an integrated approach to visual pathway diagnosis. Prog. Retin. Eye Res. **20**, 531–561 (2001).
40. Hoon, M., Okawa, H., Della Santina, L. & Wong, R. O. L. Functional architecture of the retina: development and disease. Prog. Retin. Eye Res. **42**, 44–84 (2014).
41. London, A., Benhar, I. & Schwartz, M. The retina as a window to the brain-from eye research to CNS disorders. Nat. Rev. Neurol. **9**, 44–53 (2013).
42. Silverstein, S. M., Fradkin, S. I. & Demmin, D. L. Schizophrenia and the retina: Towards a 2020 perspective. Schizophr. Res. **219**, 84–94 (2020).
43. Atilla, H. *et al.* Pattern electroretinography and visual evoked potentials in optic nerve diseases. J. Clin. Neurosci. Off. J. Neurosurg. Soc. Australas. **13**, 55–59 (2006).
44. Nightingale, S., Mitchell, K. W. & Howe, J. W. Visual evoked cortical potentials and pattern electroretinograms in Parkinson's disease and control subjects. J. Neurol. Neurosurg. Psychiatry **49**, 1280–1287 (1986).
45. Calzetti, S., Franchi, A., Taratufolo, G. & Groppi, E. Simultaneous VEP and PERG investigations in early Parkinson's disease. J. Neurol. Neurosurg. Psychiatry **53**, 114–117 (1990).
46. Krasodomska, K., Lubiński, W., Potemkowski, A. & Honczarenko, K. Pattern electroretinogram (PERG) and pattern visual evoked potential (PVEP) in the early stages of Alzheimer's disease. Doc. Ophthalmol. Adv. Ophthalmol. **121**, 111–121 (2010).
47. Heravian, J. *et al.* Simultaneous pattern visual evoked potential and pattern electroretinogram in strabismic and anisometropic amblyopia. Iran. Red Crescent Med. J. **13**, 21–26 (2011).
48. El-Shazly, A. A. E.-F., Farweez, Y. A., Hamdi, M. M. & EL-Sherbiny, N. E. Pattern Visual Evoked Potential, Pattern Electroretinogram, and Retinal Nerve Fiber Layer Thickness in Patients with Migraine during and after Aura. Curr. Eye Res. **42**, 1327–1332 (2017).
49. Bernardin, F. *et al.* Retinal ganglion cell dysfunction is correlated with disturbed visual cognition in schizophrenia patients with visual hallucinations. Psychiatry Res. **298**, 113780 (2021).
50. Bullier, J. Integrated model of visual processing. Brain Res. Rev. **36**, 96–107 (2001).
51. DeValois, R. L. & DeValois, K. K. *Spatial Vision*. (OUP USA, 1990).
52. Sheehan, D. V. *et al.* The Mini-International Neuropsychiatric Interview (M.I.N.I): The development and validation of a structured diagnostic psychiatric interview for DSM-IV and ICD-10. J. Clin. Psychiatry **59**, 22–33 (1998).
53. de Chazeron, I. *et al.* Validation of a Psycho-Sensory hAllucinations Scale (PSAS) in schizophrenia and Parkinson's disease. Schizophr. Res. **161**, 269–276 (2015).
54. World Medical Association. World Medical Association Declaration of Helsinki: ethical principles for medical research involving human subjects. JAMA **310**, 2191–2194 (2013).
55. Nelson, H. National Adult Reading Test (NART) test manual (Part 1.
56. Delis, D. C., Freeland, J., Kramer, J. H. & Kaplan, E. Integrating clinical assessment with cognitive neuroscience: construct validation of the California Verbal Learning Test. J. Consult. Clin. Psychol.

56, 123–130 (1988).

57. Godefroy, O. & GREFEX. *Fonctions exécutives et pathologies neurologiques et psychiatriques*. (2008).
58. Zimmermann, P. & Fimm, B. A test battery for attentional performance. in Applied Neuropsychology of Attention. Theory, Diagnosis and Rehabilitation 110–151 (2002).
59. Wechsler, D. & Psychological Corporation. *WAIS-III: administration and scoring manual: Wechsler Adult Intelligence Scale*. (Psychological Corporation, 1997).
60. Warrington, E. K. & James, M. *The Visual Object and Space Perception Battery: VOSP*. (Pearson, 1991).
61. Remy, I. *et al.* Impaired P100 among regular cannabis users in response to magnocellular biased visual stimuli. Prog. Neuropsychopharmacol. Biol. Psychiatry 110437 (2021) doi:10.1016/j.pnpbp.2021.110437.
62. Atkinson. Early visual development: Differential functioning of parvocellular and magnocellular pathways | Eye. https://www.nature.com/articles/eye199228.
63. Butler, P. D. *et al.* Dysfunction of early-stage visual processing in schizophrenia. Am. J. Psychiatry **158**, 1126–1133 (2001).
64. Milner, A. D. & Goodale, M. A. Two visual systems re-viewed. Neuropsychologia **46**, 774–785 (2008).
65. Jung, T.-P. *et al.* Removal of eye activity artifacts from visual event-related potentials in normal and clinical subjects. Clin. Neurophysiol. **111**, 1745–1758 (2000).
66. Schwitzer, T. *et al.* Delayed bipolar and ganglion cells neuroretinal processing in regular cannabis users: The retina as a relevant site to investigate brain synaptic transmission dysfunctions. J. Psychiatr. Res. **103**, 75–82 (2018).
67. Gunzler, D., Chen, T., Wu, P. & Zhang, H. Introduction to mediation analysis with structural equation modeling. Shanghai Arch. Psychiatry **25**, 390–394 (2013).
68. Mishkin, M., Ungerleider, L. G. & Macko, K. A. Object vision and spatial vision: two cortical pathways. Trends Neurosci. **6**, 414–417 (1983).
69. Tanaka, S., Maezawa, Y. & Kirino, E. Classification of schizophrenia patients and healthy controls using p100 event-related potentials for visual processing. Neuropsychobiology **68**, 71–78 (2013).
70. Earls, H. A., Curran, T. & Mittal, V. Deficits in Early Stages of Face Processing in Schizophrenia: A Systematic Review of the P100 Component. Schizophr. Bull. **42**, 519–527 (2016).
71. Chen, Y. *et al.* Effects of typical, atypical, and no antipsychotic drugs on visual contrast detection in schizophrenia. Am. J. Psychiatry **160**, 1795–1801 (2003).
72. Bernardin, F. *et al.* The role of the retina in visual hallucinations: A review of the literature and implications for psychosis. Neuropsychologia **99**, 128–138 (2017).
73. Diederich, N. J., Goetz, C. G. & Stebbins, G. T. Repeated visual hallucinations in Parkinson's disease as disturbed external/internal perceptions: focused review and a new integrative model. Mov. Disord. Off. J. Mov. Disord. Soc. **20**, 130–140 (2005).

74. Diederich, N. J., Stebbins, G., Schiltz, C. & Goetz, C. G. Are patients with Parkinson's disease blind to blindsight? Brain J. Neurol. **137**, 1838–1849 (2014).
75. Bernardin, F. *et al.* Retinal dysfunctions in a patient with a clinical high risk for psychosis and severe visual disturbances: A single case report. Early Interv. Psychiatry (2020) doi:10.1111/eip.13103.
76. Rapport, L. J., Millis, S. R. & Bonello, P. J. Validation of the Warrington theory of visual processing and the Visual Object and Space Perception Battery. J. Clin. Exp. Neuropsychol. **20**, 211–220 (1998).
77. Warrington, E. K. & James, M. A New Test of Object Decision: 2D Silhouettes Featuring a Minimal View. Cortex **27**, 377–383 (1991).
78. Clark, M. L., Waters, F., Vatskalis, T. M. & Jablensky, A. On the interconnectedness and prognostic value of visual and auditory hallucinations in first-episode psychosis. Eur. Psychiatry J. Assoc. Eur. Psychiatr. **41**, 122–128 (2017).
79. McCabe, M. S., Fowler, R. C., Cadoret, R. J. & Winokur, G. Symptom differences in schizophrenia with good and poor prognosis. Am. J. Psychiatry **128**, 1239–1243 (1972).
80. Mueser, K. T., Bellack, A. S. & Brady, E. U. Hallucinations in schizophrenia. Acta Psychiatr. Scand. **82**, 26–29 (1990).
81. Chouinard, V.-A. *et al.* Visual hallucinations associated with multimodal hallucinations, suicide attempts and morbidity of illness in psychotic disorders. Schizophr. Res. **208**, 196–201 (2019).
82. Schwitzer, T. *et al.* Association Between Regular Cannabis Use and Ganglion Cell Dysfunction. JAMA Ophthalmol. **135**, 54–60 (2017).
83. Pritchard, W., Sokhadze, E. & Houlihan, M. *Review Effects of nicotine and smoking on event-related potentials: A review*. (2003).
84. Kim, J. T., Yun, C. M., Kim, S.-W., Oh, J. & Huh, K. The Effects of Alcohol on Visual Evoked Potential and Multifocal Electroretinography. J. Korean Med. Sci. **31**, 783–789 (2016).

Tables

Table 1. Sociodemographic and clinical characteristics of the participants between SZ and HC group.
Data are presented as mean unless otherwise is indicated. Standard deviation is in brackets. n.s. : not significant, NA : not applicable, AUDIT : Alcohol Use Disorders Identification Test score, CAST : Cannabis Abuse Screening Test Score

	Control Group (n=29)	SZ Group (n=21)	p value of t-test
Sex : No. women/ No. men (%)	8/21 (28/72)	3/18 (14/86)	n.s.
Age (years)	25.89 [5.49]	29 [8.15]	n.s.
Education (years)	15.03 [1.57]	12.05 [1.40]	*p<0.01
AUDIT score	3.35 [2.69]	2.43 [3.41]	n.s.
Disease duration (months)	NA	94.67 [93.21]	-
Fagerström score	0 [0]	2.19 [2.77]	n.s.
CAST score	0 [0]	0.43 [1.36]	n.s.
PANSS Global	0 [0]	65.24 [13.40]	n.s.
PANSS Positive	0 [0]	14.48 [4.31]	n.s.
PANSS Negative	0 [0]	18.29 [5.57]	n.s.
PANSS General	0 [0]	32.48 [6.76]	n.s.
Chlorpromazine equivalent	0 [0]	544.55 [241.29]	n.s.
Diazepam equivalent	0 [0]	1.56 [9.64]	n.s.

Table 2. Sociodemographic and clinical characteristics of the participants between VH, AHNH and HC group. Data are presented as mean unless otherwise is indicated. Standard deviation is in brackets. n.s. : not significant, NA : not applicable, AUDIT : Alcohol Use Disorders Identification Test score, CAST : Cannabis Abuse Screening Test Score

	Control Group (n=29)	VH Group (n=9)	AHNH Group (n=12)	p value of t-test
Sex : No. women/ No. men (%)	8/21 (28/72)	1/8 (11/89)	2/10 (17/83)	n.s.
Age (years)	25.89 [5.49]	30.11 [9.47]	28.17 [7.33]	n.s.
Education (years)	15.03 [1.57]	12.11 [1.16]	12.00 [1.60]	p<0.01** (**VH/HC** and **AHNH/HC**)
AUDIT score	3.35 [2.69]	0.89 [1.45]	0.89 [4.03]	n.s.
Disease duration (months)	NA	137.33 [113.52]	72 [92.90]	n.s.
PSAS Lifetime :	NA			
Lifetime repercussion score of VH	-	12.89 [5.39]	NA	-
Lifetime repercussion score of AH	-	15.22 [8.57]	5.08 [7.63]	p<0.05
PSAS Current :	NA			
Current repercussion score of VH	-	1.22 [3.67]	NA	-
Current repercussion score of AH	-	1.78 [5.33]	1.17 [4.04]	n.s.
PANSS Global	0 [0]	64.44 [17.19]	65.83 [10.52]	n.s.
PANSS Positive	0 [0]	15.22 [5.56]	13.92 [3.23]	n.s.
PANSS Negative	0 [0]	17.11 [5.30]	19.17 [5.83]	n.s.
PANSS General	0 [0]	32.11 [9.08]	32.75 [4.79]	n.s.
Chlorpromazine equivalent	0 [0]	517.06 [187.16]	565.17 [281.60]	n.s.
Diazepam equivalent	0 [0]	0.93 [2.78]	2.54 [10.97]	n.s.

Figures

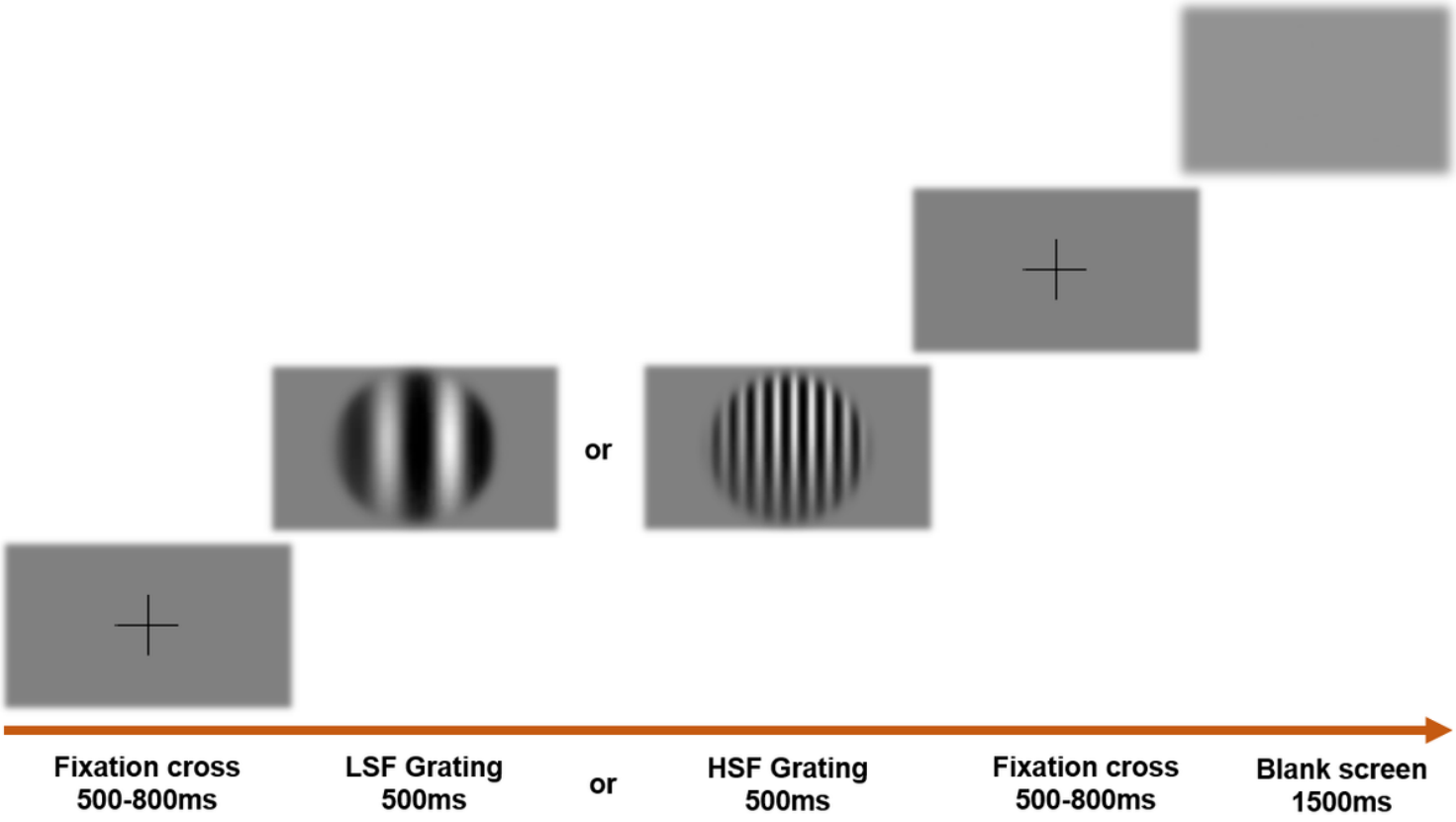

Figure 1

Representation of the experimental procedure with both LSF and HSF gratings presented during the study.

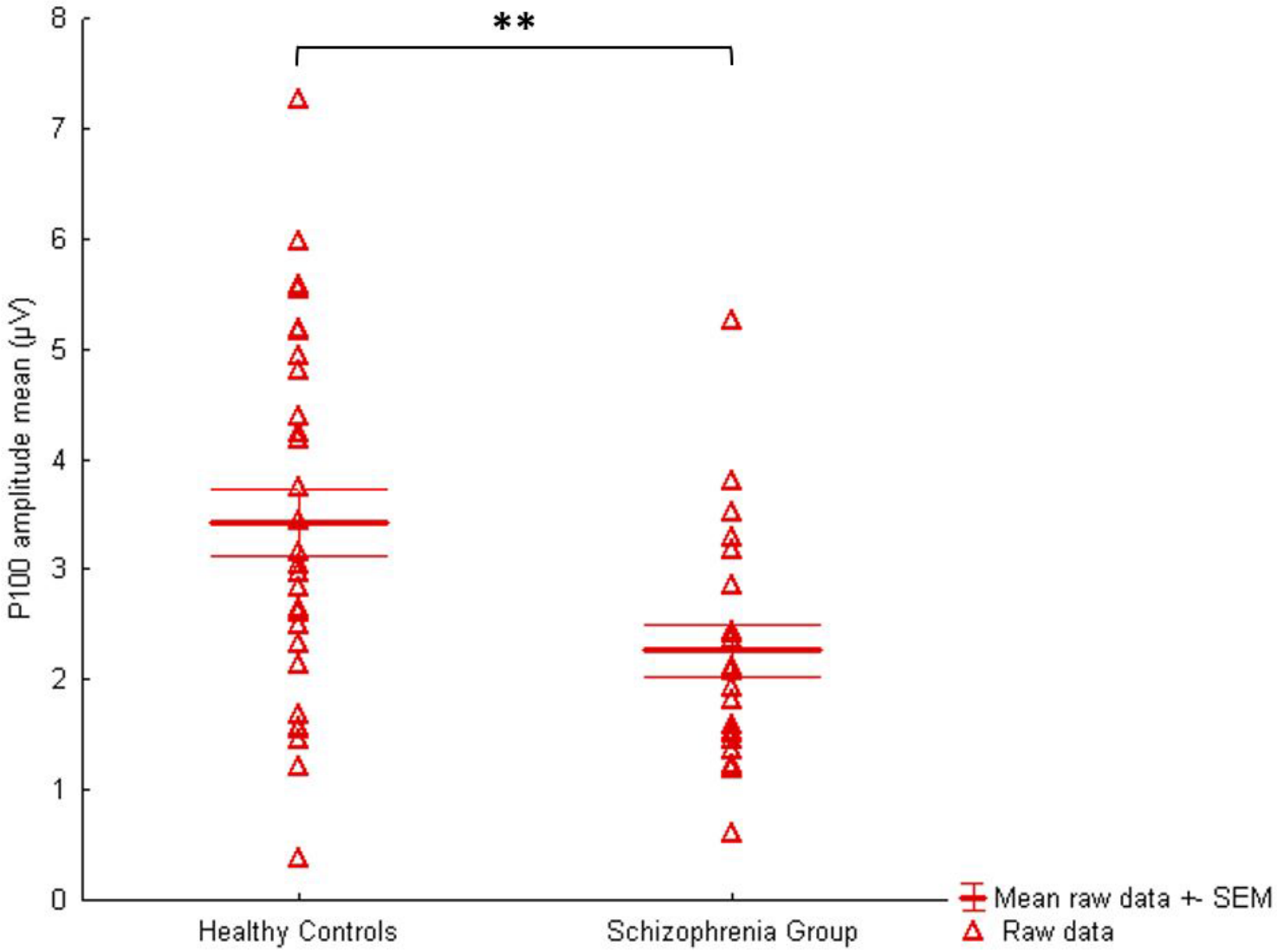

Figure 2

Main group effect on P100 amplitude between the SZ group and the HC group. Data were obtained from the average activity of the 3 pairs of interest electrodes (O_1/O_2, PO_3/PO_4, PO_7/PO_8). Means are displayed with their standard error (SEM). **p<0.01

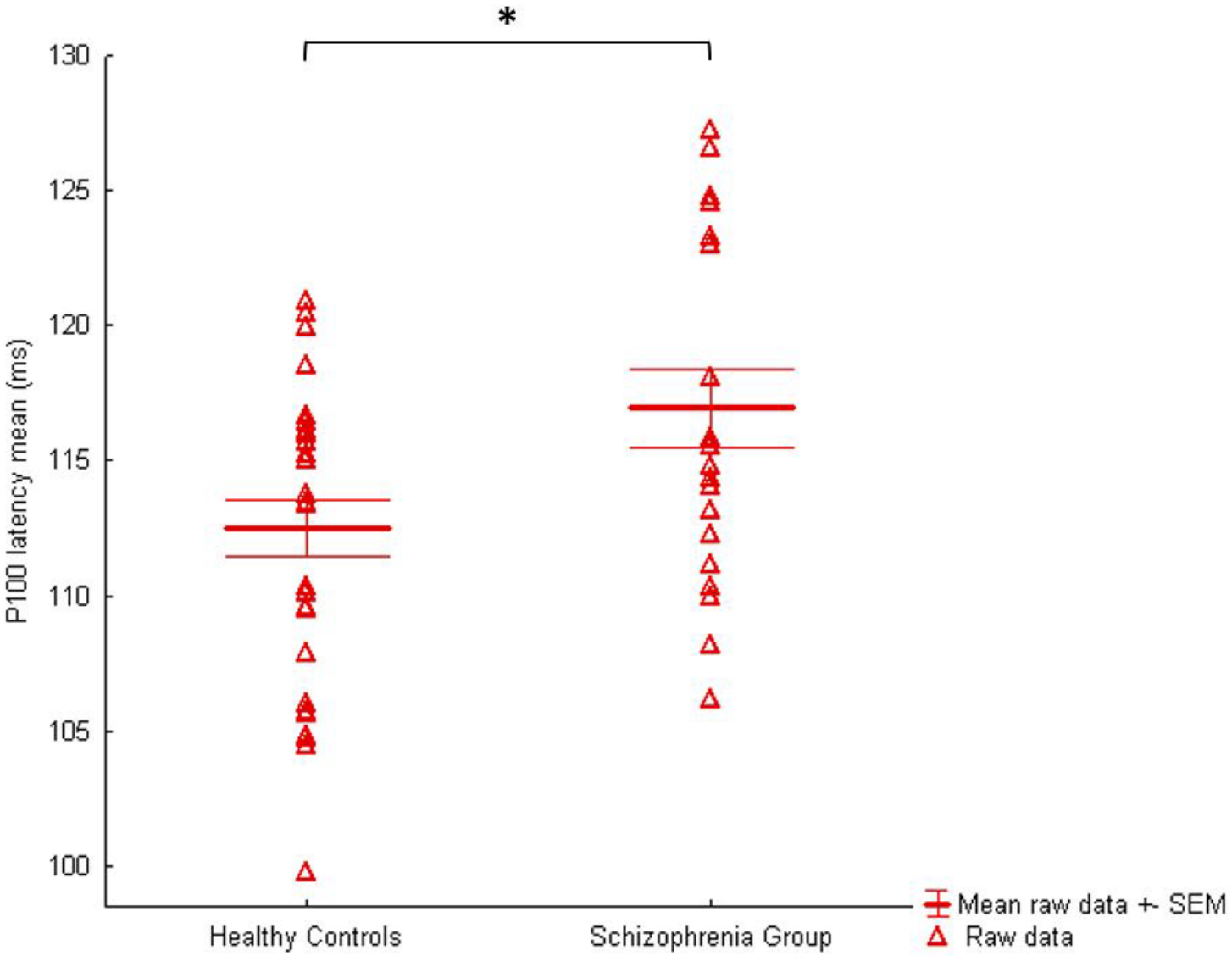

Figure 3

Main group effect on P100 latency between the SZ group and the HC group. Data were obtained from the average activity of the 3 pairs of interest electrodes (O_1/O_2, PO_3/PO_4, PO_7/PO_8). Means are displayed with their standard error (SEM). *p<0.05

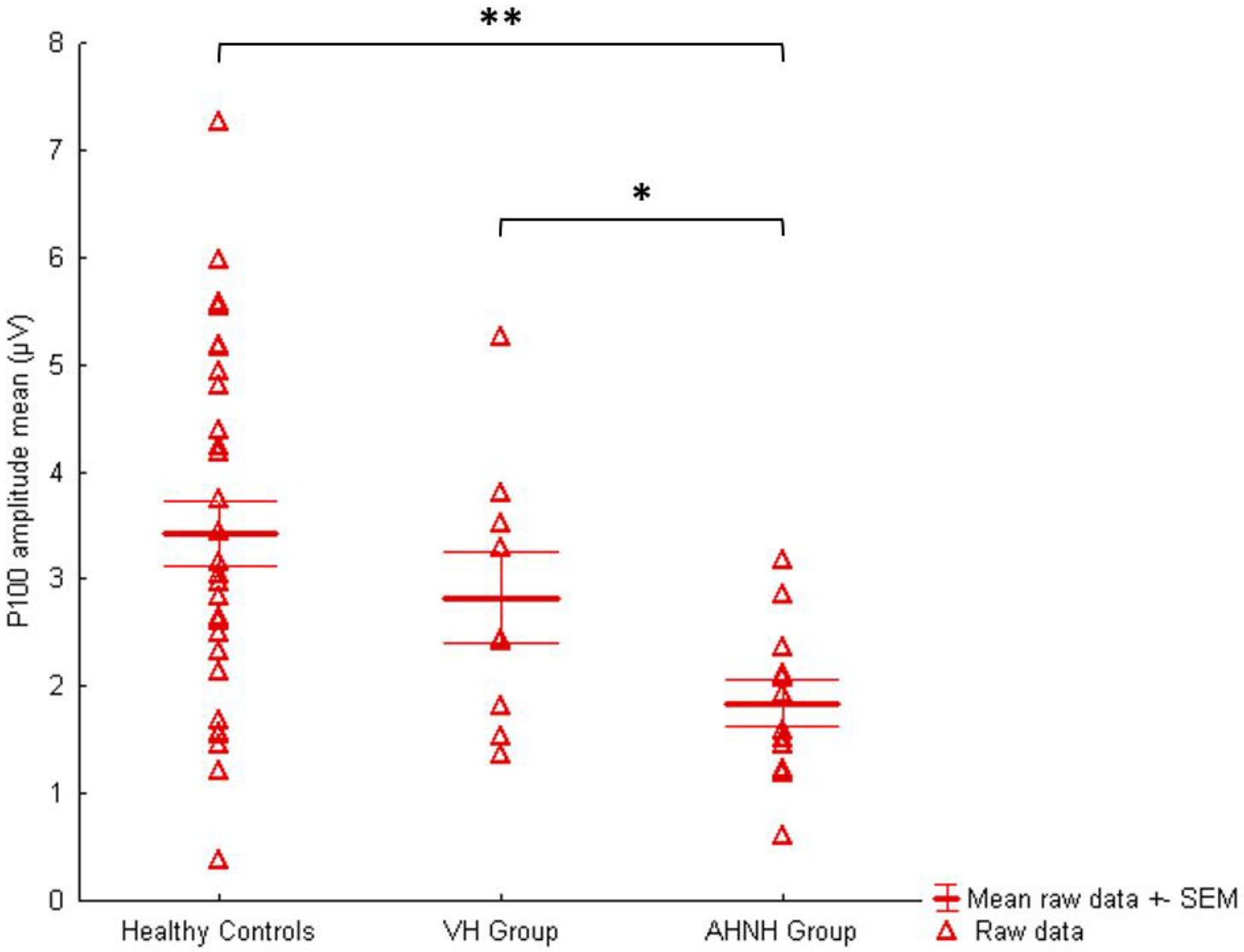

Figure 4

Main group effect on P100 amplitude between the VH group, AHNH group and the HC group. Data were obtained from the average activity of the 3 pairs of interest electrodes (O_1/O_2, PO_3/PO_4, PO_7/PO_8). Means are displayed with their standard error (SEM). The significatively is present between the AHNH group and the VH group and between the AHNH group and HC group. **p<0.01 ; *p<0.05

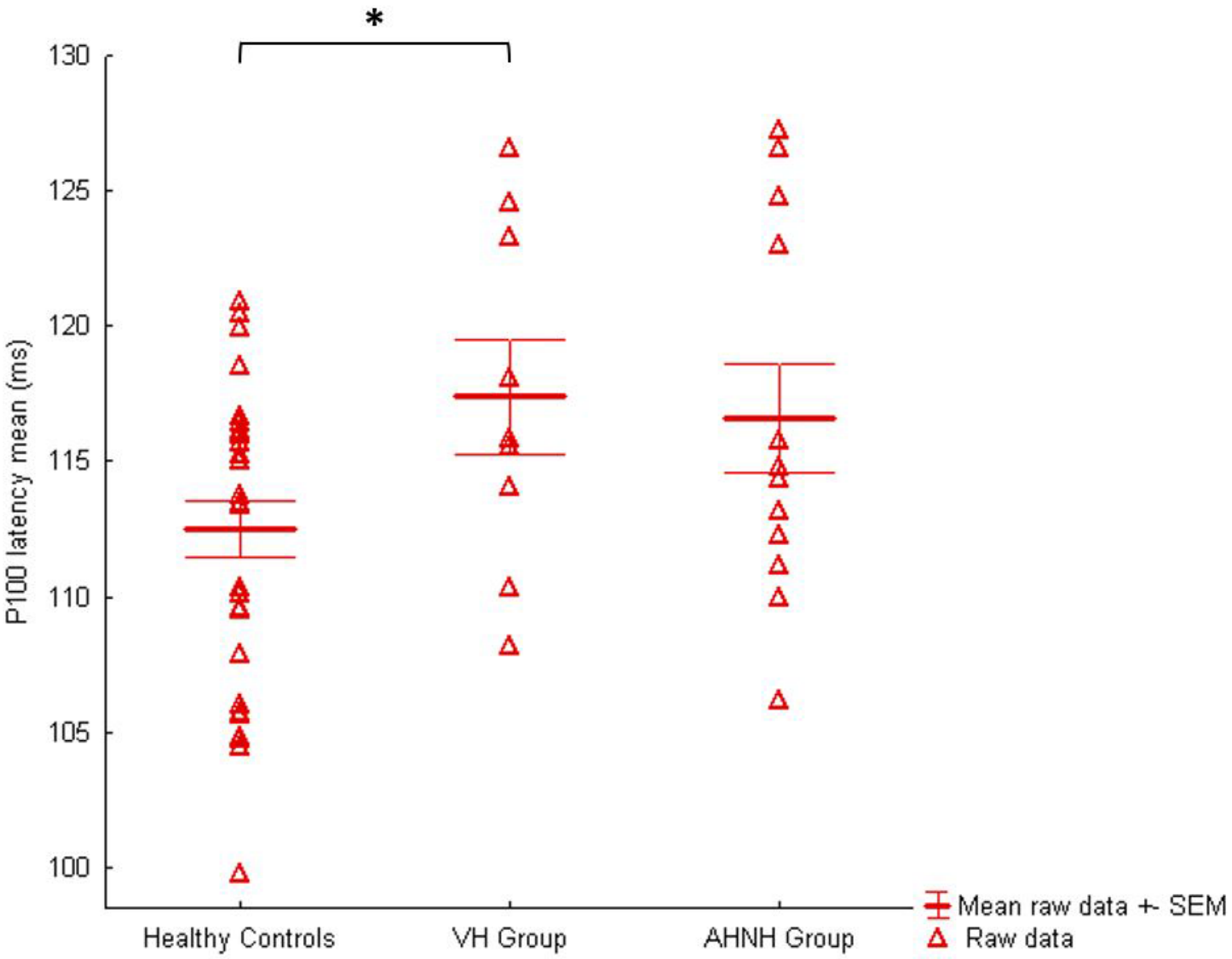

Figure 5

Main group effect on P100 latency between the VH group, AHNH group and the HC group. Data were obtained from the average activity of the 3 pairs of interest electrodes (O_1/O_2, PO_3/PO_4, PO_7/PO_8). Means are displayed with their standard error (SEM). The significatively is present between the VH group and HC group only. *p<0.05

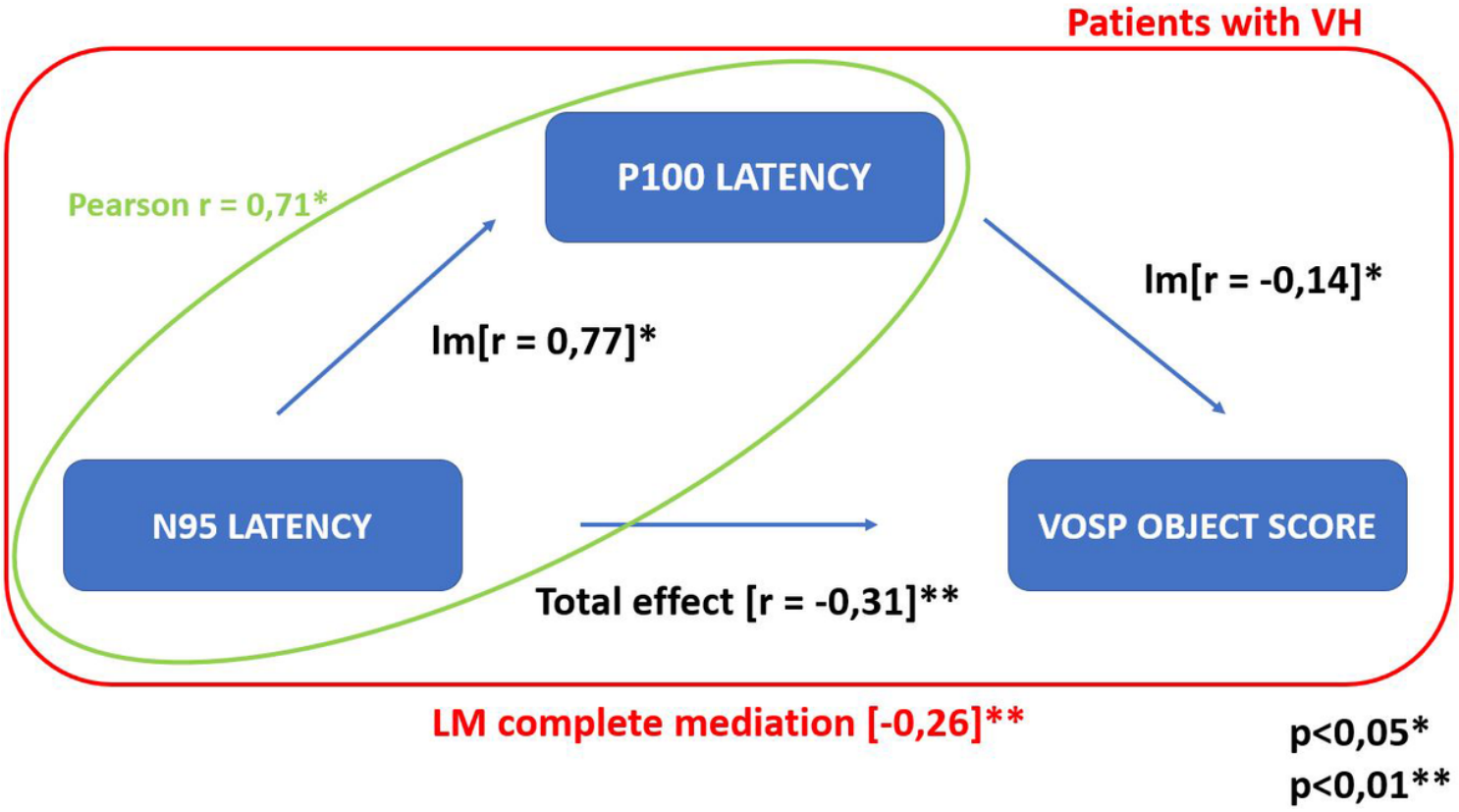

Figure 6

Mediation model (red) in the VH group. P100 latency is considered here as the mediator. Correlation test is displayed in green (Pearson), linear regression models are displayed with blue arrows. Coefficients (r) are also displayed. *p<0.05 **p<0.01

Supplementary Files

This is a list of supplementary files associated with this preprint. Click to download.

- SupplementaryResults.docx